Acoustic behavior of ordered droplets in a liquid: A phase space approach

A. L. Rivera,[1,*] M. R. Palomino,[2] M. de Icaza,[2] M. Lozada-Cassou,[1] and V. M. Castaño[2,†]
[1]*Programa de Ingeniería Molecular, Instituto Mexicano del Petróleo, Lázaro Cárdenas # 152, 07739 México, D.F., México*
[2]*Centro de Física Aplicada y Tecnología Avanzada, Universidad Nacional Autónoma de México, Apartado Postal 1-1010, 76000 Querétaro, Querétaro, México*

(Received 23 January 2004; revised manuscript received 7 July 2004; published 10 March 2005)

The transmission of an acoustical signal through a spatial arrangement consisting of a bidimensional crystal of droplets (liquid spheres) immersed into another liquid is analyzed. As a first approximation, the paraxial case is solved by considering a set of acoustical lenses which allow us to model the effect of each droplet on the signal. An expression for the Wigner distribution function that lets us evaluate the corresponding image, diffraction pattern, and even the output signal of any given paraxial input signal to that crystalline substrate is obtained, with particular emphasis on the case of an incoming plane wave. To solve the nonparaxial situation, a generalization of the concept of focal distance interpreting every sphere as a superposition of concentric rings of different radius, which permits us to find a general expression for the Wigner distribution function is proposed.

DOI: 10.1103/PhysRevE.71.036603 PACS number(s): 43.35.+d, 43.60.+d, 03.65.Fd, 61.50.Ah

I. INTRODUCTION

Wave propagation, particularly acoustic propagation through a media, is a broad and interdisciplinary field of research, in which many open questions that are scientifically sound and technologically important remain to be answered [1–4].

Among the numerous technological applications of acoustic propagation is how a surface that deflects radio waves is influenced by the dielectric constant of the material, which can be in turn affected by the water content of a material. This has been used to locate water within walls through an acoustical signal [5]. With the same logic it is possible to detect oil reservoirs and/or to asses the water content in the reservoir. Another area of growing interest is to develop more reliable exploration techniques based on sound waves that can be used to locate land mines or small, buried objects for archaeological exploration [6]. This method is similar to those used in seismic exploration, where an explosive charge is detonated and the reflected sound waves are registered by an array of receivers using a much higher frequency (i.e., with a much greater resolution) [6]. The imaging system incorporates a single-element source transducer and a receiver array, which are moved together along a linear path to collect data. To produce a three-dimensional image of an underground section, nondestructive acoustic tomography techniques [7] work illuminating the underground area of interest with acoustic plane waves of frequencies 200–3000 Hz. For each transmitted pulse, the reflected-refracted signals are received by a linear array of acoustic sensors located at a diametrically opposite point from the acoustic source line array. For a stratified underground medium and for a given depth, which is represented by a time delay in the received signal, a horizontal tomographic bidimensional image is reconstructed from the received projections. Integration of the depth-dependent sequence of cross-sectional reconstructed images provides a complete three-dimensional overview of the inspected terrain.

Photonic crystals [8] are made of periodically modulated dielectric materials, and most sonic crystals [9] are made up of materials with a periodic variation of material compositions. It has been suggested that sonic crystals could be used as sound shields and acoustic filters [10–15]. These applications mostly rely on the existence of sonic band gaps, a phenomenon discovered in a sculpture by Eusebio Sempere in Madrid [10] [sounds passing through the structure of an arrangement of polished tubes were altered, some frequencies of sound became more dominant (were reinforced) and others less so (were attenuated)]. Such band gaps were first observed in crystals where the arrangement of the atomic lattice permits only certain wavelengths of electromagnetic energy to pass. Researchers have constructed synthetic "crystals" that can filter and channel certain wavelengths of light by creating photonic band gaps [16]. Audible sound, with its longer wavelengths, responds in the same way to larger structures [10]. The experimental analysis of the acoustic transmission of a two-dimensional periodic array of rigid cylinders in air with two different geometrical configurations: square and triangular [11]. Structures creating "deaf bands" could be used by architects to design screen out or filter noise. These kind of structures were constructed by ancient peoples, the best known example being the Mayan pyramid of Kukulkan at Chichen Itza, in Mexico's Yucatan region. The odd "chirped" echo resounds from the pyramid's staircases in response to hand claps of people standing near its base [17] due to the spatially periodic design of the stone staircases that records the call of the Maya's sacred bird, the quetzal. Moreover, sonic crystals may also be used to build acoustic lenses to converge the acoustic waves. A necessary condition to be satisfied for constructing an acoustic lens is that the acoustic impedance contrast between the sonic crys-

*Currently at Centro de Física Aplicada y Tecnología Avanzada, Universidad Nacional Autónoma de México. Electronic address: analeonor@fata.unam.mx
†Electronic address: meneses@servidor.unam.mx

tal and the air should not be large; otherwise, acoustic waves will be mostly reflected. Once this condition is satisfied, the converging lens can be either convex or concave depending on whether the sound speed in the sonic crystal is smaller or greater than that in the air [18]. The theoretical explanation of this lens system built by Cervera and co-workers [18] was proposed by Gupta and Ye [19], making a numerical simulation on the focusing of acoustic waves by the sonic crystals in two refractive devices: namely, a Fabry-Perot interferometer and an acoustic convergent lens [19]. It has been shown that the shape of the crystal plays a crucial role on the quality of focusing.

Also there is enormous interest in the acoustic propagation in the interfaces of structures that model the Earth crust, a problem that shares a number of common properties with other important topics in physics, such as electron transport in mesoscopic systems and localization of photons [4] as well as phonons [3] in random media. Besides, analogies between the classical and quantum problems may lead to cross fertilization [20].

Another very powerful technique is to consider wave propagation in phase space through the Wigner distribution function (WDF). The WDF was invented by Wigner [21] to study the quantum corrections to the classical behavior of certain statistical systems described by the Boltzmann formula. From that pioneering work on the phase space representation, the WDF has proved to be a very effective tool applied to many branches of physics [22–26], in particular to signal analysis [27–30] and more specifically to acoustical signals (sound waves) [31–38] where it can be used to characterize materials [39–43]. In materials science, this characterization is relevant if properties of important engineering materials like asphaltenes, polymers, etc., are to be determined [44–46].

Here, we focus on acoustical applications, in particular on the ultrasonic characterization of materials through the transfer function of a bidimensional material. The characterization of materials is done analyzing the transmission of an acoustically known signal through the medium. This is a very complicated problem that has not been solved in general in spite of its enormous technological and scientific importance. Some approaches to solve it have been tried; in particular, acoustic-wave propagation in waveguide structures was previously studied through the WDF in the paraxial limit [34,35]. This approach leads to a ray-tracing-type algorithm fast and easy to implement, and even anisotropies in the surface of the solid could be modeled [35]. In this paper, we will start a series of works trying to analyze the transmission of acoustical signals through the WDF. As a starting point, we will consider a very simplified medium that consists of a bidimensional square net of liquid spherical droplets immersed in another liquid. We choose liquids to deal only with longitudinal waves and a bidimensional crystal due to is symmetry properties that simplified calculations. Our treatment deals with a very simplified model for acoustical problems, but it extends the WDF to the nonparaxial case and it stands the grounds for the analysis of a more realistic system in a future work.

Thus, our problem is the transmission of an acoustical signal through a substrate consisting of a bidimensional crystal of droplets (liquid spheres) immersed in a different liquid. To solve it, we will use a phase space approach via the WDF considering that the effect of the system over the signal can be modeled by the transfer function. As a first approximation we consider a paraxial signal passing through the substrate and we assume that each sphere modifies the signal as a lens. We obtain an expression for the WDF that allows us to evaluate the image, diffraction pattern, and even the output signal of any given paraxial input signal across the crystalline substrate; in particular, we consider the case of a plane-wave input. To show that this expression corresponds to the known diffraction pattern, we analyze a bidimensional square network and the continuous acoustical substrate—i.e., with a cell parameter small compared to the wavelength of the input signal. We study the nonparaxial case proposing a generalization of the concept of focal distance that allows us to interpret every sphere as a superposition of different concentric rings of various radius and then replacing each ring by an acoustical lens. With this supposition, we get a general expression for the WDF.

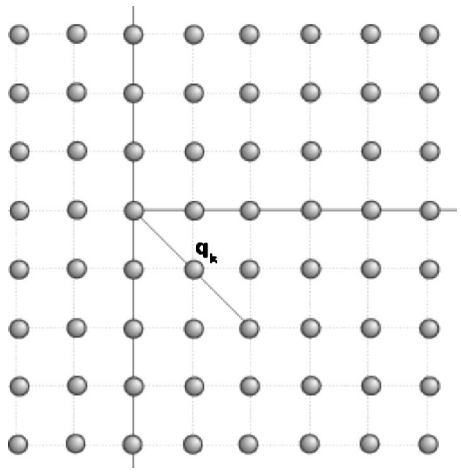

FIG. 1. Crystalline acoustical substrate consisting of lenses in the net points $\mathbf{q}_k=(k_x a, k_y a)$ with a the net parameter.

The paper is organized as follows: Section II presents the theory used in this work: the WDF (Sec. II A), the transfer function, and the so-called multislice method (Sec. II B). In Sec. III as a first approximation we study the modification of a paraxial signal by the substrate obtaining an expression for the WDF; in particular, we consider the case of a plane-wave input. In Sec. IV we study the nonparaxial case through a generalization of the concept of focal distance getting a general expression for the WDF. Section V gathers the conclusions of this paper.

II. THEORY

Our interest is the transmission of an acoustical signal through a medium with the aim of making a characterization of that media. This is a very complicated problem that we will attack considering a very simplified media that consist of a bidimensional square network of liquid spherical droplets immersed in another liquid (see Fig. 1). To solve it, we will use a phase space approach via the WDF considering

that the effect of the system over the signal can be modeled by the transfer function. To understand this treatment we will start in this section making a brief review of this subject.

A. Wigner distribution function

In a two-dimensional medium we denote the coordinates by $\mathbf{q}$ and the canonically conjugate momentum by $\mathbf{p}$. The Wigner distribution function $W_\Psi(\mathbf{q},\mathbf{p})$ of the function $\Psi(\mathbf{q})$ is defined by [21]

$$W_\Psi(\mathbf{q},\mathbf{p}) \equiv \frac{1}{2\pi}\int d\mathbf{r}\Psi*\left(\mathbf{q}-\frac{1}{2}\mathbf{r}\right)e^{-i[\mathbf{p}\cdot\mathbf{r}]}\Psi\left(\mathbf{q}+\frac{1}{2}\mathbf{r}\right) = \frac{1}{2\pi}\int d\mathbf{r}\tilde{\Psi}\left(\mathbf{p}+\frac{1}{2}\mathbf{r}\right)e^{-i[\mathbf{q}\cdot\mathbf{r}]}\tilde{\Psi}*\left(\mathbf{p}-\frac{1}{2}\mathbf{r}\right), \tag{1}$$

where $\tilde{\Psi}$ denotes the Fourier transform of Ψ, $*$ the complex conjugate, and the integrals are taken from $-\infty$ to ∞ (this is the case in all the paper, unless otherwise stated).

1. Some properties of the Wigner distribution

The complete symmetry between $\mathbf{q}$ and $\mathbf{p}$ in the former definitions of the WDF [Eq. (1)] indicates that space and momentum have equal weight in this description [47]. Due to this, the WDF can be thought as the expected value of the parity operator around $(\mathbf{q},\mathbf{p})$ in phase space [48]; i.e., the Wigner function is proportional to the overlap of $\Psi(\mathbf{q})$ with its specular image around $(\mathbf{q},\mathbf{p})$, which is a measure of "how much centered" is $\Psi(\mathbf{q})$. Note that the WDF is a four-dimensional phase space distribution function, where two dimensions correspond to real space and the other two to momentum (Fourier) space.

For numerical calculations it is very useful to notice that the WDF is the inverse Fourier transform of the autoconvolution of the signal given by the kernel [21]:

$$\mathfrak{W}(\mathbf{q},\mathbf{r}) = \Psi\left(\mathbf{q}+\tfrac{1}{2}\mathbf{r}\right)\Psi*\left(\mathbf{q}-\tfrac{1}{2}\mathbf{r}\right). \tag{2}$$

Because $\mathfrak{W}(\mathbf{q},\mathbf{r})$ is Hermitian $[\mathfrak{W}(\mathbf{q},\mathbf{r})=\mathfrak{W}*(\mathbf{q},-\mathbf{r})]$, the WDF is real [47].

To recover either the image $|\Psi(\mathbf{q})|^2$ or the diffraction pattern $|\tilde{\Psi}(\mathbf{p})|^2$ we must perform a simple projection of the WDF [21]:

$$|\Psi(\mathbf{q})|^2 = \int d\mathbf{p}W_\Psi(\mathbf{q},\mathbf{p}), \tag{3}$$

$$|\tilde{\Psi}(\mathbf{p})|^2 = \int d\mathbf{q}W_\Psi(\mathbf{q},\mathbf{p}). \tag{4}$$

If the signal or image of interest is nonstationary, the WDF gives the local spectrum centered at $\mathbf{p}$ as a function of the location [49]. Thus, the total energy of $\Psi(\mathbf{q})$ can be obtained from integration of $W_\Psi(\mathbf{q},\mathbf{p})$ over the entire phase space [50].

The original function $\Psi(\mathbf{q})$ can be recovered from the Wigner distribution up to a constant that can be obtained from the normalization condition via the next inversion theorem [30]:

$$\Psi(\mathbf{q}) = \frac{1}{\Psi*(0)}\frac{1}{2\pi}\int d\mathbf{p}W_\Psi(\mathbf{q}/2,\mathbf{p})\exp(i\mathbf{p}\cdot\mathbf{q}). \tag{5}$$

Moreover, $|W_\Psi(\mathbf{q},\mathbf{p})|\leqslant 1/(2\pi)$, and it can take negative values [47]; therefore, one cannot interpret the WDF as a classical probability function in phase space [25]. In fact, $W_\Psi(\mathbf{q},\mathbf{p})$ is strictly positive only for Gaussian wave functions [51,52]

$$\Gamma(\mathbf{q}) \equiv \left(\frac{w_1}{\pi[w_0]^2}\right)^{1/4}\exp\left\{-\frac{[\mathbf{q}-\mathbf{q}_0]^2}{2w_0}+i\mathbf{p}_0\cdot\mathbf{q}\right\}, \tag{6}$$

where w_0 is a complex number, $w_0=w_1+iw_2, w_1>0$, which determines the width of the Gaussian, $\mathbf{q}_0$ is a real vector that gives the spatial center of the distribution, and $\mathbf{p}_0$ gives the momentum center. In this case, the WDF is also Gaussian [51]:

$$W_\Gamma(\mathbf{q},\mathbf{p}) = \frac{1}{\pi}\exp\left\{-\frac{[\mathbf{q}-\mathbf{q}_0]^2}{w_1}-\frac{[w_0]^2}{w_1}[\mathbf{p}-\mathbf{p}_0]^2\right\} \times \exp\left\{\frac{2w_2}{w_1}(\mathbf{q}-\mathbf{q}_0)\cdot(\mathbf{p}-\mathbf{p}_0)\right\}. \tag{7}$$

Another interesting property is that the WDF has the same extension and is band limited as the function itself $\Psi(\mathbf{q})$ [53]. Furthermore, all the holographic information is contained in the WDF [54].

In general, the output Wigner function of any system is related to the input Wigner through [55,56]

$$W_{\Psi_{out}}(\mathbf{q},\mathbf{p}) = W_{\Psi_{in}}(a\mathbf{q}+b\mathbf{p},c\mathbf{q}+d\mathbf{p}), \tag{8}$$

where a, b, c, and d are parameters which depend on the specific system under study. As an example, a signal of wave number k traveling through the optical axis a distance z (perpendicular to the coordinates axis defined by $\mathbf{q}$) changes as

$$W_{\Psi_{out}}(\mathbf{q},\mathbf{p}) = W_{\Psi_{in}}\left(\mathbf{q}-\frac{z}{k}\mathbf{p},\mathbf{p}\right); \tag{9}$$

for a lens of focal length f, we have

$$W_{\Psi_{out}}(\mathbf{q},\mathbf{p}) = W_{\Psi_{in}}\left(\mathbf{q},\frac{\kappa}{f}\mathbf{q}+\mathbf{p}\right); \tag{10}$$

and to obtain a Fourier transform, we use

$$W_{\Psi_{out}}(\mathbf{q},\mathbf{p}) = W_{\Psi_{in}}(-\mathbf{p},\mathbf{q}). \tag{11}$$

2. Wigner distribution for a plane-wave input

To show the simplicity of calculation through the WDF in a useful problem we find the output signal of a system consisting of a lens when the input signal is a plane wave, g_{in}, given by

$$g_{in}(\mathbf{q}) = A\exp\{-i\kappa_0 z\}, \tag{12}$$

where A is the wave amplitude and κ_0 the wave vector (this signal can be optical or acoustical). In this case the WDF is

obtained substituting the input signal [Eq. (12)] into the WDF definition [Eq. (1)]:

$$W_{g_{in}}(\mathbf{q},\mathbf{p}) = AA^* * \delta(\mathbf{p}). \tag{13}$$

If this initial plane wave crosses a lens, we can use Eq. (10) to find the WDF of the outcoming wave just after the border of the lens:

$$W_{g_l}(\mathbf{q},\mathbf{p}) = W_{g_{in}}\left(\mathbf{q}, \frac{\kappa_0}{f}\mathbf{q} + \mathbf{p}\right) = AA^* * \delta\left(\frac{\kappa_0}{f}\mathbf{q} + \mathbf{p}\right). \tag{14}$$

Now, we need to propagate this outcoming wave a distance Δz (the separation between the border of the lens and the detector), using Eq. (9):

$$W_{g_{out}}(\mathbf{q},\mathbf{p}) = W_{g_l}\left(\mathbf{q} - \frac{\Delta z}{\kappa_0}\mathbf{p}, \mathbf{p}\right) = AA^* * \delta\left(\frac{\kappa_0}{f}\mathbf{q} + \left[1 - \frac{\Delta z}{f}\right]\mathbf{p}\right). \tag{15}$$

With the aid of the inversion theorem, Eq. (5), the output signal at the point z after crossing a lens results in

$$g_{out}(\mathbf{q}) = \mathcal{A}\exp\left\{-\frac{i\kappa_0}{2(f-\Delta z)}\mathbf{q}^2\right\}, \tag{16}$$

where the output amplitude is $\mathcal{A} = AA^*/[2\pi g^*_{out}(0)]$.

The traditional calculation of the output of a lens system [57] gives the same result as Eq. (16) but after longer and more complicate calculations than the ones shown here.

B. Transfer function

Any system will transform an input signal originated in the "object plane" into an output signal detected in the "image plane." As an example of a "system" we can think of a set of lenses, or a crystal, or as we will solve in this paper a bidimensional square network of liquid spherical droplets immersed into another liquid. The system can be viewed as a "black box" (called the *transfer function*) that transforms input functions (from the signal in the object plane) into output functions (signal in the image plane).

For linear systems, any input signal g_1 can be decomposed into a linear combination of pulses, so the output signal will be the linear combination of the effect of the system over each individual pulse. The decomposition can be done by using the frequency spectra of the signal obtained by Fourier transform or via Dirac δ's or plane waves or Gaussians, etc.

The effect of the system over the input signal g_1 is

$$g_2(\mathbf{q}) = \int d\mathbf{s} g_1(\mathbf{s}) h(\mathbf{q}_2, \mathbf{s}),$$

where the response to the impulse is given by

$$h(\mathbf{q}_2,\mathbf{s}) = \mathcal{L}\{\delta(\mathbf{q}_1 - \mathbf{s})\}.$$

with the operator $\mathcal{L}$ representing the effect of the system.

A system is called *spatially invariant* when a translation of the source point in the object plane produces a translation of its image in the image plane [30]. For a spatially invariant system $h(\mathbf{q}_2,\mathbf{s})$ depends only on the difference $\mathbf{q}_2 - \mathbf{s}$ and

$$g_2(\mathbf{q}) = g_1(\mathbf{q}) \circledast h(\mathbf{q}) = \int d\mathbf{s} g_1(\mathbf{s}) h(\mathbf{q}_2 - \mathbf{s}),$$

where $\circledast$ denotes the convolution operator. Applying the convolution theorem we have [58]

$$G_2(\mathbf{p}) = G_1(\mathbf{p}) \cdot \mathcal{T}(\mathbf{p}),$$

where $G_2(\mathbf{p})$ and $G_1(\mathbf{p})$ are the Fourier transforms of $g_2(\mathbf{q})$ and $g_1(\mathbf{q})$, respectively. The "transfer function" $\mathcal{T}(\mathbf{p})$ is the Fourier transform of the response to the impulse $h(\mathbf{q})$. Then, any linear system with spatial invariance can be described by convolutions or through products of their Fourier transforms.

This impulse-response approach is commonly used in signal analysis [28–30]. The multislice method was introduced in transmission electron microscopy to find the transfer function of a given sample [55]. It basically consists in decomposing the sample into a finite sum of layers (slices) of small width Δz. To solve the problem of the total transfer function we need only to determine the transfer function of each slice and consider that the output signal of one layer is the input of the next one and so on.

The transfer function of one slice is the superposition of the transmission of the wave of wavelength $\lambda = 2\pi/\kappa_0$ through a media (lens) of refractive index η [30,55,56],

$$\mathcal{T}_M(\mathbf{q}) = \exp\{i\kappa_0 \eta(\mathbf{q})\Delta z\},$$

and propagation through the layer's width Δz,

$$\mathcal{T}_{\Delta z}(\mathbf{q}) = \mathcal{T}_M(\mathbf{q})\exp\left\{-\frac{i\kappa_0\Delta z}{2}\mathbf{q}^2\right\} = \exp\left\{-i\frac{\kappa_0\Delta z}{2}[\mathbf{q}^2 - 2\eta(\mathbf{q})]\right\}. \tag{17}$$

The multislice method supposes that the acoustical substrates are characterized by different transfer functions $\mathcal{T}_M$, which depend on the material composition and of its structure through its refractive index.

The advantage of the multislice method is that each transformation can be represented by a matrix and the problem of finding the output signal of any system is reduce to simple matrix multiplication [55] instead of the complicated convolutions used it traditionally [57].

III. PARAXIAL ANALYSIS OF THE ACOUSTICAL SUBSTRATE

We consider a bidimensional square network of liquid spherical droplets immersed into another liquid (see Fig. 1). We will suppose that the effect of the spherical drops over a signal can be approximated by acoustical lenses. The use of acoustical lenses was also used by Gupta and Ye [19] to make a theoretical description of the experimental observations reported by Cervera *et al.* [18].

The transfer function of one spherical droplet in the position $\mathbf{q}_k$ is given by

$$\mathcal{T}_L(\mathbf{q};\mathbf{q}_k) = \mathcal{T}_L(\mathbf{q})\exp\left\{-\frac{i\kappa_0}{2f}[\mathbf{q}-\mathbf{q}_k]^2\right\}. \tag{18}$$

The transfer function associated with this layer of width Δz can be written using the superposition principle as

$$\mathcal{T}_T(\mathbf{q};\Delta z) = \sum_k \mathcal{T}_L(\mathbf{q};\mathbf{q}_k), \tag{19}$$

where the sum is over all the spheres inside the layer.

To obtain the WDF of $\mathcal{T}_T$ we first evaluate the autoconvolution of this transfer function [Eq. (2)] using Eqs. (18) and (19),

$$\begin{aligned}\mathfrak{W}_{\mathcal{T}_T}(\mathbf{q},\mathbf{r}) &= \mathcal{T}_T\left(\mathbf{q}+\frac{1}{2}\mathbf{r}\right)\mathcal{T}_T^*\left(\mathbf{q}-\frac{1}{2}\mathbf{r}\right)\\ &= \mathcal{T}_L\left(\mathbf{q}+\frac{1}{2}\mathbf{r}\right)\mathcal{T}_L^*\left(\mathbf{q}-\frac{1}{2}\mathbf{r}\right)\exp\left\{-\frac{i\kappa_0}{f}\mathbf{r}\cdot\mathbf{q}\right\}\\ &\times\sum_{k,l}\exp\left\{-\frac{i\kappa_0}{2f}([\mathbf{q}-\mathbf{q}_k]^2-[\mathbf{q}-\mathbf{q}_l]^2)\right\}\\ &\times\exp\left\{\frac{i\kappa_0}{2f}\mathbf{r}\cdot(\mathbf{q}_k+\mathbf{q}_l)\right\},\end{aligned}$$

and after we obtain the inverse Fourier transform of this kernel to get the WDF

$$\begin{aligned}W_{\mathcal{T}_T}(\mathbf{q},\mathbf{p}) &= \sum_{k,l}\exp\left\{-\frac{i\kappa_0}{2f}([\mathbf{q}-\mathbf{q}_k]^2-[\mathbf{q}-\mathbf{q}_l]^2)\right\}\\ &\times W_{\mathcal{T}_L}\left(\mathbf{q},\left[\mathbf{p}+\frac{\kappa_0}{f}\left(\mathbf{q}-\frac{\mathbf{q}_k+\mathbf{q}_l}{2}\right)\right]\right),\end{aligned}$$

with

$$W_{\mathcal{T}_L}(\mathbf{q},\mathbf{p}) = \frac{1}{2\pi}\int d\mathbf{r}\mathcal{T}_L\left(\mathbf{q}+\frac{1}{2}\mathbf{r}\right)\mathcal{T}_L^*\left(\mathbf{q}-\frac{1}{2}\mathbf{r}\right)e^{-i\mathbf{r}\cdot\mathbf{p}}.$$

This result corresponds to the WDF just after the bubble plane. Now we need to propagate it through a distance Δz using Eq. (9):

$$\begin{aligned}W_{\mathcal{T}_{out}}(\mathbf{q},\mathbf{p}) &= \sum_{k,l}\exp\left\{-i\frac{\kappa_0}{2f}[\mathbf{q}-\mathbf{q}_k]^2\right\}\\ &\times\exp\left\{i\frac{\kappa_0}{2f}[\mathbf{q}-\mathbf{q}_l]^2\right\}\exp\left\{-i\frac{\Delta z}{f}\mathbf{p}\cdot(\mathbf{q}_k-\mathbf{q}_l)\right\}\\ &\times W_{\mathcal{T}_L}\left(\mathbf{q}-\frac{\Delta z}{\kappa_0}\mathbf{p},\left[1-\frac{\Delta z}{f}\right]\mathbf{p}\right.\\ &\left.+\frac{\kappa_0}{f}\left[\mathbf{q}-\frac{\mathbf{q}_k+\mathbf{q}_l}{2}\right]\right).\end{aligned} \tag{20}$$

As we can see, the effect of the acoustical substrate over the signal will produce, as a WDF output, a modification of the input WDF [last term in Eq. (20)] by products of Gaussians for each droplet [first and second terms in Eq. (20)] and interference fringes (third term).

This general expression for the output WDF [Eq. (20)] will let us evaluate the image [using Eq. (3)], diffraction pattern [Eq. (4)], and even the output signal [Eq. (5)] of any given input signal that crosses the crystalline substrate.

A. Plane wave as an input signal

Under the paraxial approximation, it is a good supposition to consider that the input signal is a plane wave [Eq. (12)]; then, the WDF at the output of the acoustical substrate is obtained by substitution of Eq. (13) into Eq. (20):

$$\begin{aligned}W_{g_{out}}(\mathbf{q},\mathbf{p}) &= AA^*\sum_{k,l}\exp\left\{-i\frac{\kappa_0}{2f}[\mathbf{q}-\mathbf{q}_k]^2\right\}\\ &\times\exp\left\{i\frac{\kappa_0}{2f}[\mathbf{q}-\mathbf{q}_l]^2\right\}\\ &\times\exp\left\{-i\frac{\Delta z}{f}\mathbf{p}\cdot[\mathbf{q}_k-\mathbf{q}_l]\right\}\delta\left(\frac{\kappa_0}{f}\left[\mathbf{q}-\frac{\mathbf{q}_k+\mathbf{q}_l}{2}\right]\right.\\ &\left.+\left[1-\frac{\Delta z}{f}\right]\mathbf{p}\right).\end{aligned} \tag{21}$$

From the Wigner distribution function of the output signal, Eq. (21), we can obtain the image by simply taking the momentum marginal, Eq. (3):

$$\begin{aligned}[g_{out}(\mathbf{q})]^2 &= AA^*\sum_{k,l}\exp\left\{-i\frac{\kappa_0}{2f}([\mathbf{q}-\mathbf{q}_k]^2-[\mathbf{q}-\mathbf{q}_l]^2)\right\}\\ &\times\int d\mathbf{p}\exp\left\{-i\frac{\Delta z}{f}\mathbf{p}\cdot(\mathbf{q}_k-\mathbf{q}_l)\right\}\\ &\times\delta\left(\frac{\kappa_0}{f}\left[\mathbf{q}-\frac{\mathbf{q}_k+\mathbf{q}_l}{2}\right]+\left[1-\frac{\Delta z}{f}\right]\mathbf{p}\right).\end{aligned}$$

Due to the properties of the δ function [58], this expression reduces to the evaluation of the integrand in

$$\mathbf{p} = -\frac{\kappa_0}{2(f-\Delta z)}(2\mathbf{q}-\mathbf{q}_k-\mathbf{q}_l);$$

thus,

$$\begin{aligned}[g_{out}(\mathbf{q})]^2 &= AA^*\sum_{k}\exp\left\{-i\frac{\kappa_0}{2(f-\Delta z)}[\mathbf{q}-\mathbf{q}_k]^2\right\}\\ &\times\sum_{l}\exp\left\{i\frac{\kappa_0}{2(f-\Delta z)}[\mathbf{q}-\mathbf{q}_l]^2\right\}.\end{aligned} \tag{22}$$

Similarly, to obtain the diffraction pattern we only need to evaluate the coordinate marginal, Eq. (4), of the WDF, Eq. (21), which due to the properties of the δ function reduces to the evaluation of the integrand in

$$\mathbf{q} = \frac{\mathbf{q}_k+\mathbf{q}_l}{2} - \left(\frac{f-\Delta z}{\kappa_0}\right)\mathbf{p},$$

yielding to

$$[\tilde{g}_{out}(\mathbf{p})]^2 = AA^*\sum_{k,l}\exp\{-i\mathbf{p}\cdot(\mathbf{q}_k-\mathbf{q}_l)\}. \tag{23}$$

To find the output function we apply to Eq. (21) the inversion theorem, Eq. (5):

$$g_{out}(\mathbf{q}) = \frac{AA*}{2\pi g^{*}_{out}(0)} \sum_{k,l} \int d\mathbf{p} \exp\left\{ -i\frac{\Delta z}{f}\mathbf{p}\cdot(\mathbf{q}_k - \mathbf{q}_l) \right\} \times \exp\left\{ -i\frac{\kappa_0}{2f}\left(\left[\frac{\mathbf{q}}{2} - \mathbf{q}_k \right]^2 - \left[\frac{\mathbf{q}}{2} - \mathbf{q}_l \right]^2 \right) + i\mathbf{p}\cdot\mathbf{q} \right\} \times \delta\left(\frac{\kappa_0}{f}\left[\frac{\mathbf{q}}{2} - \frac{\mathbf{q}_k + \mathbf{q}_l}{2} \right] + \left[1 - \frac{\Delta z}{f} \right]\mathbf{p} \right).$$

Once again this simply reduces due to the properties of the δ function [58] to the evaluation of the integrand in

$$\mathbf{p} = -\frac{\kappa_0}{2(f-\Delta z)}(\mathbf{q} - \mathbf{q}_k - \mathbf{q}_l),$$

which gives

$$g_{out}(\mathbf{q}) = \mathcal{A}\sum_{k,l} \exp\left\{ -i\frac{\kappa_0}{2(f-\Delta z)}([\mathbf{q} - \mathbf{q}_k]^2 - \mathbf{q}_l^2) \right\}. \tag{24}$$

To show that this expression give us the usual diffraction pattern [57], in the next sections we will consider that the substrate is a square net.

B. Square net substrate

If we have a bidimensional square network of droplets with cell parameter a, it is convenient to locate the origin of the xy plane in the center of the net. The position of one drop in the net can be written as

$$\mathbf{q}_k = \mathbf{k}a = (k_x, k_y)a, \qquad \mathbf{q}_l = \mathbf{l}a = (l_x, l_y)a, \tag{25}$$

where k_x, k_y, l_x, and l_y are integers between $-N/2$ and $N/2$ [the net has $(N+1)^2$ drops].

After substitution of Eq. (25) into Eq. (24) we get the output signal

$$g_{out}(\mathbf{q}) = \mathcal{A}\exp\left\{ -i\frac{\kappa_0}{2(f-\Delta z)}\mathbf{q}^2 \right\} \times \sum_{k_x,k_y} \exp\left\{ -i\frac{\kappa_0 a^2}{2(f-\Delta z)}\left[\mathbf{k}^2 - 2\frac{\mathbf{q}}{a}\cdot\mathbf{k} \right] \right\} \times \sum_{l_x,l_y} \exp\left\{ i\frac{\kappa_0 a^2}{2(f-\Delta z)}\mathbf{l}^2 \right\}. \tag{26}$$

The diffraction pattern comes from Eq. (25) into Eq. (23):

$$[\tilde{g}_{out}(\mathbf{p})[^2 = AA* \sum_{k_x,k_y} \exp\{-ia\mathbf{p}\cdot\mathbf{k}\} \sum_{l_x,l_y} \exp\{ia\mathbf{p}\cdot\mathbf{l}\}. \tag{27}$$

Let us analyze the image. The image is obtained by putting Eq. (25) into Eq. (22),

$$[g_{out}(\mathbf{q})]^2 = AA* \sum_{k_x,k_y} \exp\left\{ -i\frac{\kappa_0 a^2}{2(f-\Delta z)}\left[\mathbf{k}^2 - 2\frac{\mathbf{q}}{a}\cdot\mathbf{k} \right] \right\} \times \sum_{l_x,l_y} \exp\left\{ i\frac{\kappa_0 a^2}{2(f-\Delta z)}\left[\mathbf{l}^2 - 2\frac{\mathbf{q}}{a}\cdot\mathbf{l} \right] \right\},$$

which reduces to

$$[g_{out}(\mathbf{q})]^2 = AA* \gamma\left(\frac{x}{a}\right)\gamma*\left(\frac{x}{a}\right)\gamma\left(\frac{y}{a}\right)\gamma*\left(\frac{y}{a}\right), \tag{28}$$

where $\mathbf{q}=(x,y)$ and

$$\gamma(t) \equiv \sum_n \exp\{-i\mu(n^2 - 2nt)\}, \tag{29}$$

with

$$\mu \equiv \frac{\kappa_0 a^2}{2(f-\Delta z)}. \tag{30}$$

To show that Eq. (28) produces the known diffraction pattern is enough to prove that the function γ [Eq. (29)] has a fringe pattern, which is indeed the case because γ is a periodic function of t with period

$$T = \frac{\pi}{\mu} = \frac{2\pi(f-\Delta z)}{\kappa_0 a^2},$$

i.e.,

$$\gamma(t+mT) = \sum_n \exp\{-i\mu(n^2 - 2nt)\}\exp\{2\pi inm\} = \gamma(t),$$

$$m = 0, \pm 1, \pm 2, \ldots .$$

To find the order of the peaks of the diffraction pattern we write the function γ as an Airy function [58] and take the limit when t goes to 0:

$$\lim_{t\to 0}\gamma(t) = \lim_{t\to 0}\sum_{n=-N}^{N} \exp\{-i\mu n^2\}\exp\{2i\mu nt\} = \lim_{t\to 0}\frac{\exp\{2i\mu t(N+1)\} - \exp\{2i\mu t(-N)\}}{\exp\{2i\mu t\} - 1} = \lim_{t\to 0}\frac{\sin[\mu t(2N+1)]}{\sin[\mu t]} = 2N+1,$$

with N the number of liquid drops in one direction. If we have a square crystal, the order of the diffraction pattern peaks is $(2N+1)^2$.

C. Continuous acoustical substrate

When the net parameter a of the acoustical substrate is small compared to the wavelength of the input wave we can

approximate the summations in Eq. (28) by integrals. For that we have

$$\begin{aligned}\gamma(t) &= \sum_n \exp\{-i\mu(n^2-2nt)\} \\ &= \exp\{i\mu t^2\}\sum_{n=-N/2}^{n=N/2}\exp\{-i\mu(n-t)^2\}\Delta n \\ &\approx \exp\{i\mu t^2\}\int_{-N/2}^{N/2} dn\,\exp\{-i\mu(n-t)^2\} \\ &= \sqrt{\frac{\pi}{2\mu}}e^{i\mu t^2}\int_{-(\sqrt{2\mu/\pi})[N/2+t]}^{(\sqrt{2\mu/\pi})[N2-t]} e^{-i(\pi/2)u^2}du \\ &= \sqrt{\frac{\pi}{2\mu}}e^{i\mu t^2}\mathcal{C}(u)\begin{bmatrix}\sqrt{\frac{2\mu}{\pi}}\left[\frac{N}{2}-t\right], \\ -\sqrt{\frac{2\mu}{\pi}}\left[\frac{N}{2}+t\right],\end{bmatrix} \end{aligned} \tag{31}$$

where $\mathcal{C}(u)$ is the Cornu integral.

If we have a very big crystal (infinite length), it is enough to make $N\to\infty$ in the limits of the integrals.

To get the image we substitute Eq. (31) into Eq. (28):

$$[g_{out}(\mathbf{q})]^2 = \frac{AA^*\pi^2(f-\Delta z)^2}{\kappa_0^2 a^4}\mathcal{C}(u)\begin{bmatrix}x_2 \\ x_1\end{bmatrix}\mathcal{C}(u)*\Bigg]_{x_1}^{x_2} \times\mathcal{C}(u)\begin{bmatrix}y_2 \\ y_1\end{bmatrix}\mathcal{C}(u)*\Bigg]_{y_1}^{y_2}, \tag{32}$$

with

$$x_1 = -\sqrt{\frac{2\mu}{\pi}}\left(\frac{N}{2}+\frac{x}{a}\right), \quad x_2 = \sqrt{\frac{2\mu}{\pi}}\left(\frac{N}{2}-\frac{x}{a}\right),$$

$$y_1 = -\sqrt{\frac{2\mu}{\pi}}\left(\frac{N}{2}+\frac{y}{a}\right), \quad y_2 = \sqrt{\frac{2\mu}{\pi}}\left(\frac{N}{2}-\frac{y}{a}\right).$$

In the case of a finite crystal, the image is given by products of $\mathcal{C}$ functions, with a modulus oscillating between maxima and minima producing light and dark fringes (diffraction pattern).

IV. NONPARAXIAL BEAM TREATMENT

The former solution for a bidimensional net of droplets was done supposing that each spherical droplet can be treated as a lens and that the rays are paraxial ones; i.e., they are near to the optical axis [57]. To solve the problem of finding the outcoming signal crossing the acoustical substrate of Fig. 1, in this section we study nonparaxial rays, proposing a generalization to the concept of focal distance [39], and we construct the WDF using this definition.

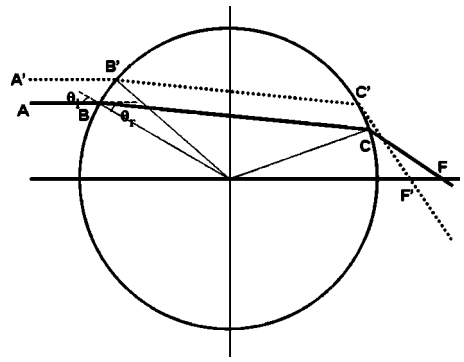

FIG. 2. An acoustical incident ray AB in a sphere of radius R, parallel to the optical axis, will suffer two refractions, one at the sphere entrance in $B(r_i)$ and another at the exit in $C(r_i)$, to cross finally the optical axis in the focal point $\mathcal{F}(r_i)$.

A. Nonparaxial focal distance

Traditionally [57], the *focal distance* f of a lens is defined as the distance between the center of the lens and the point where parallel rays converge after crossing the lens. Under the paraxial approximation, the focal distance is independent of the angle between the rays and optical axis. Indeed, this condition implies that paraxial rays not only make a small angle with the optical axis, but also that they are close to this axis.

For a given nonparaxial ray incident over a sphere, the *optical axis* is the parallel line to this axis that crosses the center of the sphere (see Fig. 2). We define the *focal distance* as the distance between the sphere center and the point where the incident ray cuts the optical axis. The *sphere plane* is the perpendicular plane to the optical axis that intercepts the sphere center playing a role like a lens. Once we have an optical axis assigned, a parallel ray to this axis cannot cross the sphere; then, we say that the ray has an infinite focal distance. We will consider the focal distance as positive if the convergence point is on the back with respect to the sense of advance of the ray.

A beam of parallel rays with the same distance r to the optical axis has the same focal distance $f(r)$. This set of incident rays constitutes the surface of a cylinder of radius r, the center of which coincides with the optical axis of the sphere. If we consider a set of parallel rays between two cylinders of radius r and $r+\Delta r$, with Δr small, then all these rays converge in the same point, at a distance $f(r)$. We can describe this "tube" of rays as an intersection with the sphere plane, which is the annular zone between r and $r+\Delta r$.

Let us consider an acoustical ray AB incident over a sphere of radius R parallel to the optical axis (see Fig. 2). This ray will suffer two refractions, one when it enters in B and another when it goes out in C until it crosses the optical axis in the focal point $\mathcal{F}$. The position in the optical axis of the point $\mathcal{F}$ depends on the position of the point B, which can be described through the angle θ_i or through the distance to the axis r_i. For paraxial rays, $r_i \approx 0$ and $\mathcal{F}=\mathcal{F}(r_i)$ must be independent of r_i. If we denote by θ_r the refraction angle (in agreement with Fig. 2), the focal distance is given by

$$\mathcal{F}(r_i) = R\{\cos[2\theta_r - \theta_i(r_i)] + \sin[2\theta_r - \theta_i(r_i)] \times \cot[2\theta_i(r_i) - 2\theta_r]\}, \quad (33)$$

where θ_r and θ_i fulfill Snell's refraction law:

$$\frac{\sin\theta_i}{\sin\theta_r} = \frac{c_i}{c_r} = \frac{\eta_r}{\eta_i}, \quad (34)$$

with c_i and c_r the sound velocities inside and outside the sphere, respectively, and η_i and η_r the corresponding refractive indexes.

Equations (33) and (34) give for each θ_i a focal distance $\mathcal{F}(\theta_i(r_i))$ that lets us interpret the sphere as a superposition of concentric rings of different radius. The one analyzed in Fig. 2 is the ring with incident angle in the sphere θ_i and $\theta_i + \Delta\theta_i$. This ring behaves like a lens with a focal distance $\mathcal{F}(\theta_i(r_i))$ given by Eq. (33).

B. Transformation of the Wigner distribution function for the nonparaxial system

In Sec. II A we saw that the WDF of a signal crossing a lens of focal distance f is transformed via Eq. (10) followed by free propagation from the lens until the point where we want to calculate the acoustical field [Eq. (9)] [55,56]:

$$W_{g_{l_p}}(\mathbf{q},\mathbf{p}) = W_g\left(\mathbf{q} - \mathbf{p}\frac{\Delta z}{k_0}, \mathbf{p}\left[1 - \frac{\Delta z}{f}\right] + \frac{k_0}{f}\mathbf{q}\right). \quad (35)$$

This result has two approximations: rays with small tilt with respect to the optical axis and near to it—i.e., paraxial rays.

To obtain a better approximation than the one given by Eq. (35), let us consider a plane wave that propagates initially through the optical axis z—i.e., that satisfies the paraxial conditions. Let us suppose that the wave insides over a sphere of radius $R < R_0$ and that it is effectively a plane within a cylinder of radius R. The part of the wave that it is not in the annular section between R and R_0 does not have contact inside over the sphere. The part of the wave inside the cylinder of radius R has a focal distance given by Eq. (33). Let us notice that when we decompose an incident plane wave into rings, in agreement with the correspondent rays, then the optical paths do not coincide, losing their coherence. Then we propose the next approximation to the sphere problem:

$$W_{g_{S_p}}(\mathbf{q},\mathbf{p}) = \int_0^{R_0} \mathrm{d}r\left[\frac{2\pi r}{\pi R_0^2}\right] \times W_g\left(\mathbf{q} - \mathbf{p}\frac{\Delta z}{k_0}, \mathbf{p}\left[1 - \frac{\Delta z}{\mathcal{F}(r)}\right] + \frac{k_0}{\mathcal{F}(r)}\mathbf{q}\right), \quad (36)$$

where $\mathcal{F}(r)$ is given by Eq. (33).

For the bidimensional square net of the liquid spherical droplets immerse into a different liquid shown in Fig. 1; the WDF will be given by [obtained in an analogous way as Eq. (20)]

$$W_{\mathcal{T}_{out}}(\mathbf{q},\mathbf{p}) = \frac{2}{R_0^2}\int_0^{R_0} \mathrm{d}r\, r \times \sum_k \exp\left\{-\frac{i}{\mathcal{F}(r)}\left(\Delta z\mathbf{p}\cdot\mathbf{q}_k + \frac{\kappa_0}{2}[\mathbf{q} - \mathbf{q}_k]^2\right)\right\} \times \sum_l \exp\left\{\frac{i}{\mathcal{F}(r)}\left(\Delta z\mathbf{p}\cdot\mathbf{q}_l + \frac{\kappa_0}{2}[\mathbf{q} - \mathbf{q}_l]^2\right)\right\} \times W_g\left(\mathbf{q} - \frac{\Delta z}{\kappa_0}\mathbf{p}, \left[1 - \frac{\Delta z}{\mathcal{F}(r)}\right]\mathbf{p} + \frac{\kappa_0}{\mathcal{F}(r)}\left[\mathbf{q} - \frac{\mathbf{q}_k + \mathbf{q}_l}{2}\right]\right). \quad (37)$$

The effect of the acoustical substrate over the signal will produce, as an output WDF, simply the product of the input WDF evaluated in a transformed phase space point [last term in Eq. (37)] by products of Gaussians $(\exp\{i\kappa_0|\mathbf{q} - \mathbf{q}_j|^2/[2\mathcal{F}(r)]\})$ and interference fringes $(\exp\{i\Delta z\mathbf{p}\cdot\mathbf{q}_j/\mathcal{F}(r)\})$ for each droplet summed over all the spheres inside the substrate and integrated over all the space. The term $\mathcal{F}(r)$ takes into account the nonparaxial character of the medium.

C. Plane waves through a nonparaxial system

In the case of a plane-wave input [Eq. (12), then the WDF at the output of the acoustical substrate is obtained by substitution of Eq. (13) into Eq. (37):

$$W_{\mathcal{T}_{out}}(\mathbf{q},\mathbf{p}) = \frac{2}{R_0^2}\int_0^{R_0} \mathrm{d}r \sum_{k,l} r\exp\left\{-i\frac{\Delta z}{\mathcal{F}(r)}\mathbf{p}\cdot(\mathbf{q}_k - \mathbf{q}_l)\right\} \times \exp\left\{-i\frac{\kappa_0}{2\mathcal{F}(r)}([\mathbf{q} - \mathbf{q}_k]^2 - [\mathbf{q} - \mathbf{q}_l]^2)\right\} \times \delta\left(\left[1 - \frac{\Delta z}{\mathcal{F}(r)}\right]\mathbf{p} + \frac{\kappa_0}{\mathcal{F}(r)}\left[\mathbf{q} - \frac{\mathbf{q}_k + \mathbf{q}_l}{2}\right]\right), \quad (38)$$

where $\mathcal{F}(r)$ is given by Eq. (33).

The main modification of the output WDF of an incoming plane wave crossing a nonparaxial system [Eq. (38)] and a paraxial one [Eq. (21)] is that the focal distance has to be modified via Eq. (33) and then integrated over all the radius of each droplet, but we still have the typical interference fringes characteristic of a periodic array.

V. CONCLUSIONS

In this paper the transmission of a signal through an acoustical substrate consisting of a bidimensional crystal of droplets (liquid spheres) embedded into another liquid was theoretically analyzed. We consider liquids to deal only with longitudinal waves. At a first approximation we solve the paraxial problem considering an acoustical lens to model the effect of each drop over the signal. Using the transfer function technique developed in Sec. II B, we found a general

expression for the Wigner distribution function of the output signal [Eq. (20)] showing that the input WDF will be modified by products of Gaussians and interference fringes. As an example, we consider the case of a plane-wave input [Eq. (12)] obtaining from the WDF [Eq. (21)]: the image [Eq. (22)], the diffraction pattern [Eq. (23)], and even the output signal [Eq. (24)]. Taking the specific case of a square lattice we demonstrate the traditional periodicity from a diffraction pattern due to the spatial periodicity of the substrate. In the case of a crystal with a small net parameter we can approximate the sums by integrals, letting us follow a diffraction analysis similar to the one of Fresnel. To solve the nonparaxial situation we make a generalization of the concept of focal distance [Eq. (33)] that allows us to interpret the sphere as a superposition of concentric rings of different radius. With this new definition we rewrite the Wigner distribution function of the output signal [Eq. (37)]; in particular, we consider the case of an incoming plane wave [Eq. (38)]. In addition to the basic physics behind our results, which represent a simpler method for evaluation of the transmission of an acoustical signal through a medium, they can be relevant for producing novel acoustical and/or photonic materials.

[1] P. Sebbah, *Waves and Imaging Through Complex Media* (Kluwer, Dordrecht, 2001).
[2] D. S. Wiersma, P. Bartolini, A. Lagendijk, and R. Righini, Nature (London) **390**, 671 (1997).
[3] S. He and J. D. Maynard, Phys. Rev. Lett. **57**, 3171 (1986).
[4] P. E. Wolf and G. Maret, Phys. Rev. Lett. **55**, 2696 (1985).
[5] W. M. Healy and E. van Doorn, ASHRAE Trans. (to be published).
[6] C. H. Frazier, N. Cadalli, D. C. Munson, and W. D. O'Brien, J. Acoust. Soc. Am. **108**, 147 (2000).
[7] W. A. Younis, S. stergiopoulos, D. Havelock, and J. Grodski, J. Acoust. Soc. Am. **111**, 2117 (2002).
[8] J. Joannopoulos, R. Meade, and J. Winn, *Photonic Crystals* (Princeton University Press, Princeton, 1995).
[9] J. P. Dowling, J. Acoust. Soc. Am. **91**, 2539 (1992).
[10] R. Martínez-Sala, J. Sancho, J. V. Sánchez, V. Gómez, J. Llinares, and F. Meseguer, Nature (London) **378**, 241 (1995).
[11] J. V. Sánchez-Pérez, D. Caballero, R. Martinez-Sala, C. Rubio, J. Sánchez-Dehesa, F. Meseguer, J. Llinares, and F. Galvez, Phys. Rev. Lett. **80**, 5325 (1998).
[12] Y. Y. Chen and Zhen Ye, Phys. Rev. Lett. **87**, 184301 (2001).
[13] D. Caballero, J. Sánchez-Dehesa, C. Rubio, R. Martinez-Sala, J. V. Sánchez-Pérez, F. Meseguer, and J. Llinares, Phys. Rev. E **60**, R6316 (1999).
[14] L. Sanchis *et al.*, J. Acoust. Soc. Am. **109**, 2598 (2001).
[15] M. S. Kuswahs, Appl. Phys. Lett. **70**, 3218 (1997).
[16] A. Blanco, E. Chomski, S. Grabtchak, M. Ibisate, S. John, S. W. Leonard, C. Lopez, F. Meseguer, H. Miguez, J. P. Mondia, G. A. Ozin, O. Toader, and H. M. van Driel, Nature (London) **405**, 437 (2000).
[17] Alan Hall, Sci. Am. (Int. Ed.) **279**(6), 26 (1998).
[18] F. Cervera, L. Sanchis, J. V. Sánchez-Pérez, R. Martínez-Sala, C. Rubio, F. Meseguer, C. López, D. Caballero, and J. Sánchez-Dehesa, Phys. Rev. Lett. **88**, 023902 (2002).
[19] B. C. Gupta and Z. Ye, Phys. Rev. E **67**, 036603 (2003).
[20] A. L. Rivera, N. M. Atakishiyev, S. M. Chumakov, and K. B. Wolf, Phys. Rev. A **55**, 876 (1997).
[21] E. P. Wigner, Phys. Rev. **40**, 749 (1932).
[22] I. Stewart *et al.*, *The Symmetry Perspective: From Equilibrium to Chaos in Phase Space and Physical Space* (Birkhauser, Boston, 2002).
[23] D. Dragoman, in *Progress in Optics XXXVII*, edited by E. Wolf (Elsevier, Amsterdam, 1997).
[24] V. V. Dodonov, O. V. Man'ko, and V. I. Man'ko, Phys. Rev. A **49**, 2993 (1994).
[25] H. W. Lee, Phys. Rep. **259**, 147 (1995).
[26] Y. S. Kim and M. E. Noz, *Phase Space Picture of Quantum Mechanics* (World Scientific, Singapore, 1991).
[27] B. Boashash, *Time Frequency Signal Analysis and Processing: A Comprehensive Reference* (Elsevier, Amsterdam, 2003).
[28] V. C. Chen, *Time-Frequency Transforms for Radar Imaging and Signal Analysis* (Artech House, New York, 2002).
[29] W. Mecklenbrauker *et al.*, *The Wigner Distribution: Theory and Applications in Signal Processing* (Elsevier, Amsterdam, 1997).
[30] L. Cohen, *Time-Frequency Analysis* (Prentice-Hall, Englewood Cliffs, NJ, 1995).
[31] R. Latif, E. Aassif, A. Moudden, and B. Faiz, Meas. Sci. Technol. **14**, 1063 (2003).
[32] M. Palmese, A. Bozzo, S. Jesus, J. Onofre, P. Picco, and A. Trucco, Acta. Acust. Acust. **88**, 653 (2002).
[33] N. Baydar and A. Ball, Mech. Syst. Signal Process. **15**, 1091 (2001).
[34] J. Salo, K. Bjorknas, J. Fagerholm, A. T. Friberg, and M. M. Salomaa, Proc.-IEEE Ultrason. Symp. **1**, 147 (1997).
[35] J. Fagerholm, A. T. Friberg, J. Huttunen, D. P. Morgan, and M. M. Salomaa, IEEE Trans. Ultrason. Ferroelectr. Freq. Control **44**, 505 (1997).
[36] D. C. Reid, A. M. Zoubir, and B. Boashash, J. Acoust. Soc. Am. **102**, 207 (1997).
[37] G. C. Gaunaurd and H. C. Strifors, Proc. IEEE **84**, 1231 (1996).
[38] J. Hasegawa and K. Kobayashi, IEICE Trans. Fundamentals **E77-A**, 1867 (1994).
[39] M. R. Palomino, MSc thesis, UNAM, México, 1997.
[40] A. V. Dobrynin and M. Rubinstein, J. Phys. Chem. B **107**, 8260 (2003).
[41] R. Latif, E. Aassif, A. Moudden, and B. Faiz, Acta. Acust. Acust. **89**, 253 (2003).
[42] L. Demeio, L. Barletti, A. Bertoni, P. Bordone, and C. Jacoboni, Physica B **314**, 104 (2002).
[43] L. Bessais, C. Djega-Mariadassou, and J. M. Greneche, J. Magn. Magn. Mater. **226**, 1564 (2001).
[44] M. Srećković, N. Ivanović, O. Zizić, and S. Bojanić, J. Electron. Mater. **32**, 208 (2003).
[45] S. Lepri, R. Livi, and A. Politi, Phys. Rep. **377**, 1 (2003).
[46] G. Cannelli, R. Cantelli, F. Cordero, and F. Trequattrini, Phys. Rev. B **55**, 14 865 (1997).

[47] J. E. Moyal, Proc. Cambridge Philos. Soc. **45**, 99 (1949).
[48] A. Royer, Phys. Rev. A **15**, 449 (1977).
[49] H. O. Bartelt, K. H. Brenner, and A. H. Lohmann, Opt. Commun. **32**, 32 (1980).
[50] M. Hillery, R. F. O'Connell, M. O. Scully, and E. P. Wigner, Phys. Rep. **106**, 121 (1984).
[51] R. L. Hudson, Rev. Math. Phys. **6**, 249 (1974).
[52] F. Soto and P. Claverie, J. Math. Phys. **24**, 97 (1983).
[53] W. Schempp, in *Lie Methods in Optics*, edited by J. Sanchez-Mondragon and K. B. Wolf, Lecture Notes in Physics, Vol. 250 (Springer-Verlag, Heidelberg, 1986).
[54] K. B. Wolf and A. L. Rivera, Opt. Commun. **144**, 36 (1997).
[55] V. M. Castaño, G. Vázquez-Polo, and R. Gutiérrez Castrejón, Scanning Microsc. Suppl. **6**, 415 (1992).
[56] R. Gutiérrez Castrejón and V. M. Castaño, Optik (Stuttgart) **91**, 24 (1992).
[57] M. Born and E. Wolf, *Principles of Optics*, 6th ed. (Pergamon, Oxford, 1984).
[58] K. B. Wolf, *Integral Transforms in Science and Engineering* (Plenum, New York, 1979).